

## Comparison of human skin opto-thermal response to near-infrared and visible laser irradiations: a theoretical investigation

Tianhong Dai<sup>1</sup>, Brian M Pikkula<sup>1</sup>, Lihong V Wang<sup>2</sup> and Bahman Anvari<sup>1</sup>

<sup>1</sup> Department of Bioengineering, Rice University, Houston, TX 77251, USA

<sup>2</sup> Department of Biomedical Engineering, Texas A&M University, College Station, TX 77843, USA

E-mail: anvari@rice.edu

Received 4 July 2004

Published 8 October 2004

Online at [stacks.iop.org/PMB/49/4861](http://stacks.iop.org/PMB/49/4861)

doi:10.1088/0031-9155/49/21/002

### Abstract

Near-infrared wavelengths are absorbed less by epidermal melanin, and penetrate deeper into human skin dermis and blood than visible wavelengths. Therefore, laser irradiation using near-infrared wavelengths may improve the therapeutic outcome of cutaneous hyper-vascular malformations in moderately to heavily pigmented skin patients and those with large-sized blood vessels or blood vessels extending deeply into the skin. A mathematical model composed of a Monte Carlo algorithm to estimate the distribution of absorbed light, numerical solution of a bio-heat diffusion equation to calculate the transient temperature distribution, and a damage integral based on an empirical Arrhenius relationship to quantify the tissue damage was utilized to investigate the opto-thermal response of human skin to near-infrared and visible laser irradiations in conjunction with cryogen spray cooling. In addition, the thermal effects of a single continuous laser pulse and micropulse-composed laser pulse profiles were compared. Simulation results indicated that a 940 nm wavelength induces improved therapeutic outcome compared with a 585 and 595 nm wavelengths for the treatment of patients with large-sized blood vessels and moderately to heavily pigmented skin. On the other hand, a 585 nm wavelength shows the best efficacy in treating small-sized blood vessels, as characterized by the largest laser-induced blood vessel damage depth compared with 595 and 940 nm wavelengths. Dermal blood content has a considerable effect on the threshold incident dosage for epidermal damage, while the effect of blood vessel size is minimal. For the same macropulse duration and incident dosage, a micropulse-composed pulse profile results in higher peak temperature at the basal layer of skin epidermis than an ideal single continuous pulse profile.

## 1. Introduction

Pulsed dye lasers at the wavelengths of 585 and 595 nm have been the common choices for the treatment of cutaneous hyper-vascular malformations such as telangiectasia (Buscher *et al* 2000), port wine stain (Nguyen *et al* 1998, Ho *et al* 2002) and haemangiomas (Hohenleutner *et al* 2001). However, clinical studies have shown that complete blanching of the lesions is not commonly achieved, and multiple treatments are usually required to obtain optimal blanching (Nguyen *et al* 1998, Ho *et al* 2002, Hohenleutner *et al* 2001). Moreover, in some cases, patients are unresponsive to pulsed dye laser irradiation (Lanigan 1998). The possible reasons for these limited therapeutic outcomes are the limited light penetration depth in large-sized blood vessels as well as in blood vessels extending deeply into the skin dermis, and subsequent non-uniform heating in various blood vessel layers. Additionally, as epidermal melanin, mainly located at the basal layer of epidermis (dermo–epidermal junction), competes with subsurface targeted blood vessels in the absorption of laser light, a large number of the patients, namely those with high melanin concentration skin types, are still excluded from the laser treatment due to significant light absorption by the epidermal melanin, which can lead to persistent hyper-pigmentation and textural changes to the skin (Ashinoff and Geronemus 1992).

Near-infrared wavelengths are absorbed less by epidermal melanin, and penetrate deeper into skin dermis and blood than visible wavelengths (Kaudewitz *et al* 2001). Therefore, laser irradiation using near-infrared wavelengths may improve the therapeutic outcome of cutaneous hyper-vascular malformations in moderately to heavily pigmented skin patients and those with large-sized blood vessels or blood vessels extending deeply into the skin. Since blood absorption coefficients of near-infrared wavelengths are lower than those of visible wavelengths, higher incident dosages are required to generate intravascular temperatures required for blood vessel coagulation, and skin surface cooling techniques such as cryogen spray cooling (CSC) (Anvari *et al* 1995) may be required to protect the skin epidermis. Using a mathematical model composed of a Monte Carlo algorithm to estimate the distribution of absorbed light followed by numerical solution of a bio-heat diffusion equation to calculate the transient temperature distribution and a damage integral based on an empirical Arrhenius relationship to quantify the tissue damage, we investigated the opto-thermal response of human skin to near-infrared wavelength laser irradiation in conjunction with CSC (cryogen type R134A, boiling point  $-26.2$  °C at atmospheric pressure), and compared it with that to pulsed dye laser irradiation emitting visible light.

For treating large-sized blood vessels, long laser pulse durations that match the thermal relaxation time of the blood vessels are believed to be more effective (Nelson *et al* 1995). Newly developed pulsed dye lasers deliver long macro laser pulses (1.5–40 ms) that are composed of a chain of micro pulses. This type of laser pulse profile is still a reasonable approximation to a true long single pulse as long as the intervals between the micro pulses are shorter than the thermal relaxation time of targeted blood vessel, so heat is still confined within the blood vessel during irradiation. In this theoretical study, the thermal effects of single continuous laser pulse and micropulse-composed laser pulse profiles were also compared.

## 2. Materials and methods

### 2.1. Human skin geometry

The geometry to simulate human skin with hyper-vascular malformations consisted of a 60  $\mu\text{m}$  thick epidermis with a 15  $\mu\text{m}$  thick basal melanin layer, and a 1940  $\mu\text{m}$  thick dermis

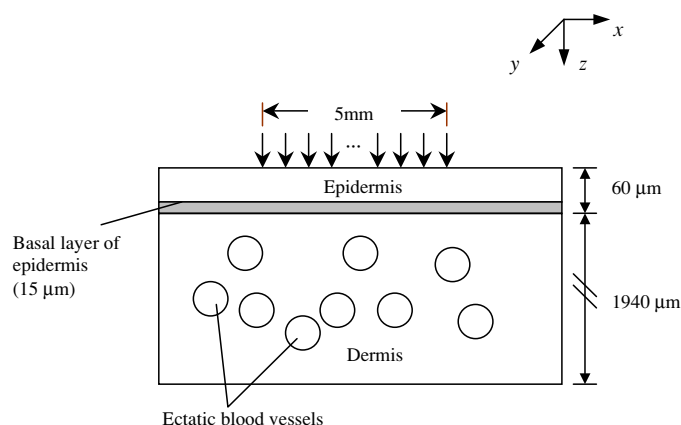


**Figure 1.** Geometry model of human skin with hyper-vascular malformation.

embedded with discrete ectatic blood vessels (figure 1). According to the data reported by Jacques (1998), the volume fractions of melanosomes based on the whole skin epidermis are 1.3–6.3%, 11–16% and 18–43% for lightly, moderately and heavily pigmented skin, respectively. As a result, the corresponding average values are 3.8%, 13.5% and 30.5%. In the present study, we considered that the epidermal melanin only filled the basal layer of epidermis, and the remaining areas of epidermis were melaninless. For the skin geometry used here (i.e., 15  $\mu\text{m}$  thick basal layer of epidermis and 45  $\mu\text{m}$  thick melaninless layer of epidermis), the volume fractions of melanosomes in the basal layer of epidermis were set to be 15, 50 and 95% for lightly, moderately and heavily pigmented skin, respectively. The former two values were obtained by multiplying the corresponding values based on the whole epidermis by 4 (60  $\mu\text{m}/15 \mu\text{m}$ ). The third value was adjusted to 95%, as  $30.5\% \times 4 > 100\%$ . The blood vessels were assumed to be straight cylinders running parallel to the  $y$  direction and with infinite lengths. The number of blood vessels and their sizes could be varied. The haematocrit (hct) of the whole blood was 45%. The beam spot was assumed to be a square flat-top profile with a size of 5 mm  $\times$  5 mm.

## 2.2. Optical properties of human skin

In the present study, effects of near-infrared wavelength 940 nm and two visible wavelengths 585 and 595 nm were investigated. Three near-infrared wavelengths 810, 940 and 1064 nm are currently available and used for therapeutic purposes. Recent studies (Dai *et al* 2004, Kaudewitz *et al* 2002) showed that 940 nm wavelength is superior to 810 and 1064 nm in terms of the ratio of the absorbed light by targeted blood vessel to that by the basal layer of epidermis. The determination of skin optical properties at various wavelengths is detailed as follows.

**2.2.1. Optical properties of blood.** Oxy-haemoglobin ( $\text{HbO}_2$ ) was used throughout the study to represent blood chromophores. The absorption and scattering coefficients of blood,  $\mu_{a,\text{blood}}$  and  $\mu_{s,\text{blood}}$ , at 585 and 595 nm for hct = 45% were scaled from the data reported by Kienle and Hibst (1995), which were for hct = 40% originally:

$$\begin{aligned} \mu_{a,\text{blood}}(\lambda = 585 \text{ and } 595 \text{ nm, hct} = 45\%) \\ = \mu_{a,\text{blood}}(\lambda = 585 \text{ and } 595 \text{ nm, hct} = 40\%) \times (45/40) \end{aligned} \quad (1)$$

$$\begin{aligned}\mu_{s,\text{blood}}(\lambda = 585 \text{ and } 595 \text{ nm, hct} = 45\%) \\ = \mu_{s,\text{blood}}(\lambda = 585 \text{ and } 595 \text{ nm, hct} = 40\%) \times (45/40)\end{aligned}\quad (2)$$

where  $\lambda$  is the wavelength in nm. The absorption coefficients of blood  $\mu_{a,\text{blood}}$  for hct = 45% at 940 nm were reported by Jacques (1998).

The reduced scattering coefficient of blood  $\mu'_{s,\text{blood}}$  at 810 nm was reported by Roggan *et al* (1995) as 6.6 and 3.9  $\text{cm}^{-1}$  for 40% hct. Thus, the mean value of  $\mu'_{s,\text{blood}}(\lambda = 810 \text{ nm, hct} = 40\%) = 5.25 \text{ cm}^{-1}$  was applied to 810  $\mu\text{m}$  wavelength for 40% hct. We assumed the corresponding anisotropy factor  $g$  to be 0.99. Therefore, the scattering coefficient of blood at 810 nm wavelength for hct = 40% was

$$\mu_{s,\text{blood}}(\lambda = 810 \text{ nm, hct} = 40\%) = \mu'_{s,\text{blood}}(\lambda = 810 \text{ nm, hct} = 40\%)/(1 - g) \approx 525 \text{ cm}^{-1}.\quad (3)$$

A previous study (Roggan *et al* 1999) indicated that scattering and absorption increase linearly with hct if hct < 50%. As a result, for hct = 45%, scattering coefficient of blood at 810 nm wavelength was

$$\begin{aligned}\mu_{s,\text{blood}}(\lambda = 810 \text{ nm, hct} = 45\%) = \mu_{s,\text{blood}}(\lambda = 810 \text{ nm, hct} = 40\%) \\ \times (45/40) \approx 590 \text{ cm}^{-1}.\end{aligned}\quad (4)$$

The scattering coefficient of blood at 940 nm wavelength was derived from the relationship that the scattering coefficient decreases for wavelengths above 800 nm with approximately  $\lambda^{-1.7}$  (Roggan *et al* 1999), and the scattering coefficient at 810 nm served as the reference value. The anisotropy factors  $g$  were set to be 0.99 as well for the near-infrared wavelength 940 nm (Graaff *et al* 1993), and 0.995 for 585 and 595 nm wavelengths (Kienle and Hibst 1995).

**2.2.2. Optical properties of skin epidermis.** Based on the skin model geometry used in the present study, skin epidermis is composed of two layers: a melaninless epidermis layer and a melanin-filled basal layer. The absorption coefficient of melaninless epidermis  $\mu_{a,\text{epi}}(\text{cm}^{-1})$  was given by (Jacques 1998)

$$\mu_{a,\text{epi}} = \mu_{a,\text{base}} = 0.244 + 85.3 \exp[-(\lambda - 154)/66.2]\quad (5)$$

where  $\mu_{a,\text{base}}$  is the baseline absorption coefficient of skin (i.e., absorption coefficient of melaninless epidermis or bloodless dermis) (Jacques 1998).

The total optical absorption coefficient of the basal layer of epidermis  $\mu_{a,\text{ebas}}$  depends on a minor baseline skin absorption  $\mu_{a,\text{base}}$  and a dominant melanin absorption due to the melanosomes in the basal layer:

$$\mu_{a,\text{ebas}} = f_{\text{mel}} \cdot \mu_{a,\text{mel}} + (1 - f_{\text{mel}})\mu_{a,\text{base}}\quad (6)$$

where  $f_{\text{mel}}$  is the volume fraction of melanosomes in the basal layer of epidermis;  $\mu_{a,\text{mel}}(\text{cm}^{-1})$  is the absorption coefficient of a single melanosome, and was calculated as (Jacques 1998)

$$\mu_{a,\text{mel}} = 6.6 \times 10^{11} \cdot \lambda^{-3.33}.\quad (7)$$

Scattering coefficients of melaninless epidermis and basal layer of epidermis were approximated to be the same, and calculated as (Jacques 1998)

$$\mu_s = (2 \times 10^5 \cdot \lambda^{-1.5} + 2 \times 10^{12} \cdot \lambda^{-4})/(1 - g)\quad (8)$$

**Table 1.** Human skin optical properties used in the present study.

Wavelength (nm)	Optical properties	Epidermis	Basal layer (L) <sup>a</sup>	Basal layer (M) <sup>b</sup>	Basal layer (H) <sup>c</sup>	Dermis	Blood
940	$\mu_a$ (cm <sup>-1</sup> )	0.24	12.66	41.62	78.85	0.26	6.79
	$\mu_s$ (cm <sup>-1</sup> )	105.57	105.57	105.57	105.57	105.57	458.58
	$g$	0.91	0.91	0.91	0.91	0.91	0.99
595	$\mu_a$ (cm <sup>-1</sup> )	0.35	57.38	190.45	361.53	0.45	48.4
	$\mu_s$ (cm <sup>-1</sup> )	148.69	148.69	148.69	148.69	148.69	523.12
	$g$	0.8	0.8	0.8	0.8	0.8	0.995
585	$\mu_a$ (cm <sup>-1</sup> )	0.37	60.71	201.50	382.52	0.8	214.9
	$\mu_s$ (cm <sup>-1</sup> )	156.06	156.06	156.06	156.06	156.06	525.38
	$g$	0.8	0.8	0.8	0.8	0.8	0.995

<sup>a</sup> L: light pigmentation.

<sup>b</sup> M: moderate pigmentation.

<sup>c</sup> H: heavy pigmentation.

where  $\mu_s$  is the scattering coefficient (cm<sup>-1</sup>). The values of  $g$  were assumed to be 0.91 for the near-infrared wavelengths 940 nm (Graaff *et al* 1993), and 0.8 for visible wavelengths 585 and 595 nm (Kienle and Hibst 1995).

**2.2.3. Optical properties of skin dermis.** Absorption coefficient of dermis  $\mu_{a,der}$  is expressed as

$$\mu_{a,der} = f_{blood} \cdot \mu_{a,blood} + (1 - f_{blood})\mu_{a,base} \quad (9)$$

where  $f_{blood}$  is the volume fraction of blood in the dermis (the blood content of ectatic blood vessels is not taken into account here). A typical value of  $f_{blood}$  is 0.2% where a homogeneous distribution of blood in the dermis is assumed (Jacques 1998). Scattering coefficient and anisotropy factor of the dermis were considered to be the same as those values of epidermis (Jacques 1998). In summary, the optical properties used in the present study are depicted in table 1.

### 2.3. Mathematical model

Mathematical model consisted of a Monte Carlo algorithm (Wang *et al* 1995) to calculate the distribution of absorbed light in the skin, a bio-heat conduction model to calculate the transient temperature distribution, and a damage integral based on an empirical Arrhenius relationship to quantify the thermal damage to the tissue (Agah *et al* 1994). The bio-heat conduction equation was in the following format:

$$k \left[ \frac{\partial T^2(x, z, t)}{\partial^2 x} + \frac{\partial T^2(x, z, t)}{\partial^2 z} \right] + S(x, z) = \rho C \frac{\partial T(x, z, t)}{\partial t} \quad (10)$$

where  $k$  is the thermal conductivity (W m<sup>-1</sup> K<sup>-1</sup>),  $T(x, z, t)$  is the skin temperature (K),  $x$  is the lateral distance with the origin at the beam centre (m),  $z$  is the depth into skin with the origin at the skin surface,  $t$  is the time (s),  $S(x, z)$  is the heat source term (W m<sup>-3</sup>),  $\rho$  is the density (kg m<sup>-3</sup>),  $C$  is the specific heat capacity (J kg<sup>-1</sup> K<sup>-1</sup>). The thermo-physical properties of human skin used in the study were density  $\rho = 1200$  kg m<sup>-3</sup>, specific heat capacity  $C = 3600$  J kg<sup>-1</sup> K<sup>-1</sup>, thermal conductivities  $k = 0.26, 0.53, 0.53$  W m<sup>-1</sup> K<sup>-1</sup> for epidermis, dermis and blood, respectively (Duck 1990). We did not account for the latent heat of water vaporization.

**Table 2.** Values used in the bio-heat conduction model (Tunnell *et al* 2003a).

Time period	Heat transfer coefficient (W m <sup>-2</sup> °C <sup>-1</sup> )	Temperature of the medium <sup>a</sup> right above the skin surface (°C)
Spurt application	4000	-50
Cryogen pool residence	3000	-26
Rewarming	10	25

<sup>a</sup> The medium refers to cryogen film during the spurt duration and cryogen pool residence interval, and it refers to air during the rewarming period.

Each simulation was carried out for 1000 000 photons. The initial skin temperature was assumed to be 33 °C. Convection surface boundary condition (Incropera and Dewitt 2001) was used for the solution of the bio-heat conduction model:

$$-k \left. \frac{\partial T(x, z, t)}{\partial z} \right|_{z=0} = h[T_{\text{med}} - T(x, z, t)|_{z=0}] \quad (11)$$

where  $T_{\text{med}}$  is the temperature of the medium above the skin surface (K),  $h$  is the heat transfer coefficient between the skin surface and the above medium (W m<sup>-2</sup> K<sup>-1</sup>). If not specially mentioned, the contours of the laser pulses at all wavelengths and all pulse durations were assumed to be continuous in the present study.

Previous studies (Torres *et al* 1999, Aguilar *et al* 2001, Tunnell *et al* 2002) indicated that when CSC is applied to skin, there exist three successive different time intervals: (1) cryogen application period; (2) cryogen pool residence: liquid cryogen remains on the skin surface for a period of time (tens to hundreds of milliseconds depends on cryogen spurt duration) after the termination of cryogen spurt; (3) rewarming: time period after the complete evaporation of liquid cryogen film. The values of  $h$  and  $T_{\text{med}}$  for different time intervals are listed in table 2 (Tunnell *et al* 2003a).

Thermal damage to skin was quantified by the damage integral  $\Omega(x, z, t)$  based on an empirical Arrhenius relationship:

$$\Omega(x, z, \tau) = A \int_0^\tau \exp \left[ -\frac{E}{RT(x, z, t)} \right] dt \quad (12)$$

with  $A = 1.8 \times 10^{51} \text{ s}^{-1}$ , damage process activation energy  $E = 327\,000 \text{ J mol}^{-1}$  (Weaver and Stoll 1969), and universal gas constant  $R = 8.314 \text{ J mol}^{-1} \text{ K}^{-1}$ . When the damage integral  $\Omega(x, z, \tau)$  reaches 1, then 63% of the tissue is assumed to be damaged. This limit was taken to be the criterion for irreversible damage. The outputs of the model were the absorbed light profiles, temperature profiles and maps of damaged area within the skin. The computation of the damage integral was stopped about four thermal relaxation times of the targeted blood vessels after the termination of laser irradiation. In four thermal relaxation times, the temperatures of the blood vessels would be cooled down below the coagulation temperature and no additional thermal damage would be expected.

### 3. Results

#### 3.1. Verification of human skin optical properties

In order to verify the validity of the human skin optical properties used in the present theoretical study (calculated by the formulae in section 2.2, and depicted in table 1), we compared the

**Table 3.** Simulation results of threshold incident dosages for epidermal damage  $D_{th}$  in response to 595 nm laser irradiation in conjunction with a 100 ms cryogen spurt. Laser pulse duration: 1.5 ms.

Skin pigmentation	$f_{mel}$ (%) <sup>a</sup>	$f'_{mel}$ (%) <sup>b</sup>	$D_{th}$ (J cm <sup>-2</sup> ) <sup>c</sup>
Light	15	3.8	33
Moderate	50	12.5	16.8
Heavy	95	23.8	12.7

<sup>a</sup>  $f_{mel}$ : Volume fraction of melanosomes based on the basal layer of epidermis.

<sup>b</sup>  $f'_{mel}$ : Volume fraction of melanosomes based on the whole epidermis.

<sup>c</sup>  $D_{th}$ : Threshold incident dosage for epidermal damage.

**Table 4.** *In vivo* experimental results of threshold incident dosages for epidermal damage  $D_{th}$  in response to 595 nm laser irradiation in conjunction with a 100 ms cryogen spurt. Laser pulse duration: 1.5 ms.

Sample no.	Skin type <sup>b</sup>	$D_{th}$ (J cm <sup>-2</sup> )	$D_{th,av}$ (J cm <sup>-2</sup> ) <sup>c</sup>
1	II	>30 <sup>d</sup>	
2	II	>30 <sup>d</sup>	>30
3	II	30	
4	III	12	
5	III	22	20.7
6	III	28	
7	V	8	
8	V	14	9
9	V	5	

<sup>a</sup> Unpublished data of an *in vivo* study conducted by our group.

<sup>b</sup> Fitzpatrick skin classification (Fitzpatrick 1988).

<sup>c</sup>  $D_{th,av}$ : Average threshold incident dosage for epidermal damage.

<sup>d</sup> No epidermal damage was observed at 30 J cm<sup>-2</sup>, which was the highest incident dosage used in the experiment.

simulation results of threshold incident dosages for epidermal damage ( $D_{th}$ ) in response to 595 nm laser irradiation (table 3) with the experimental results of an *in vivo* study of normal human skin of nine subjects irradiated at the same wavelength (table 4) conducted by our group. The threshold incident dosage for epidermal damage was defined as the maximum incident dosage that did not induce epidermal damage. The laser pulse duration used in the *in vivo* study was 1.5 ms, and the cryogen spurt duration 100 ms. For normal human skin, the blood content of the dermis was assumed to be 0.2% in the simulation (Jacques 1998).

Fitzpatrick skin types I–II, III–IV and V–VI were considered respectively as lightly, moderately and heavily pigmented skin types (Tunnell *et al* 2003b). For lightly pigmented skin, only type II was obtained in the *in vivo* experiments (table 4), and the average value of the threshold incident dosage for epidermal damage  $D_{th,av}$  was higher than 30 J cm<sup>-2</sup>. The corresponding predicted threshold incident dosage for epidermal damage for lightly pigmented skin was 33 J cm<sup>-2</sup>. For moderately pigmented skin, the experimental and simulation results were 20.7 and 16.8 J cm<sup>-2</sup>, respectively. Considering that the experimental results on moderately pigmented skin were only from type III skin and not type IV skin (for which the value is expected to be lower), the prediction can be considered reasonable. For heavily pigmented skin, the predicted value (12.7 J cm<sup>-2</sup>) is 41% higher than the experimental result (9 J cm<sup>-2</sup>). One of the possible reasons for this discrepancy is the large range of the melanin concentration in heavily pigmented skin: 18–43% based on the whole epidermis (Jacques 1998).

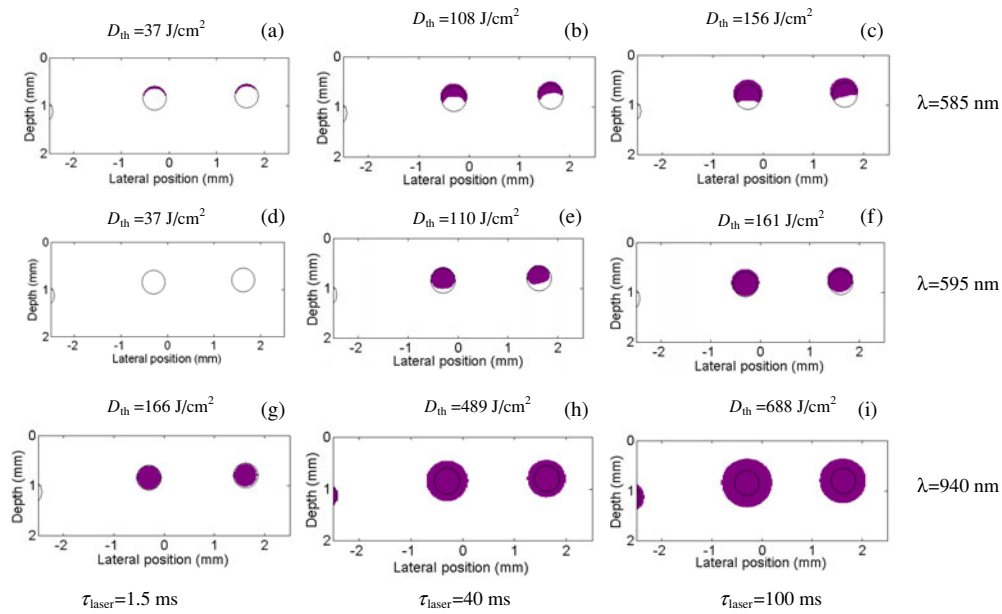


**Figure 2.** Comparison of thermal damage to blood vessel in response to 585 nm ((a), (b) and (c)), 595 nm ((d), (e) and (f)) and 940 nm ((g), (h) and (i)) irradiations in lightly pigmented skin at the threshold incident dosages for epidermal damage  $D_{th}$ . Blood vessel diameter: 500  $\mu\text{m}$ . Cryogen spurt duration: 100 ms. Laser pulse durations: 1.5 ms ((a), (d) and (g)), 40 ms ((b), (e) and (h)) and 100 ms ((c), (f) and (i)). Circled areas: blood vessels; dark areas: damaged regions of blood vessels.

### 3.2. Blood vessel damage—large-sized blood vessels

**3.2.1. Lightly pigmented skin.** The simulation results of laser-induced vascular damage maps of 500  $\mu\text{m}$  diameter blood vessels in lightly pigmented skin irradiated by 585, 595 and 940 nm wavelengths at the threshold incident dosages for epidermal damage  $D_{th}$  are shown in figure 2. The dark areas indicate the damaged regions in the skin. The value of  $D_{th}$  is dependent upon laser wavelength, laser pulse duration, cryogen spurt duration, skin pigmentation level and dermal blood content. The cryogen spurt duration  $\tau_{CSC}$  was 100 ms. With the laser pulse duration  $\tau_{laser} = 1.5$  ms, slight damage was predicted in the most superficial layer of the blood vessels at 585 nm wavelength (figure 2(a)), no blood vessel damage occurred at 595 nm wavelength (figure 2(d)), while the two blood vessels were completely damaged at 940 nm wavelength (figure 2(g)). When the  $\tau_{laser}$  was increased to 40 and 100 ms, the blood vessels were partially or considerably damaged at 585 and 595 nm (figures 2(b), (c), (e) and (f)), and completely damaged at 940 nm (figures 2(h) and (i)). Perivascular damage (dark areas outside the blood vessel circles) occurred at 585 nm when the laser pulse durations were 40 and 100 ms (figures 2(b) and (c)), and at 595 nm when  $\tau_{laser} = 100$  ms (figure 2(f)), while the blood vessels were still not completely damaged. Perivascular damage can also be observed when  $\lambda = 940$  nm and  $\tau_{laser} = 40$  and 100 ms (figures 2(h) and (i)). However, a further investigation showed that when  $\lambda = 940$  nm and  $\tau_{laser} = 40$  and 100 ms, the blood vessels could be completely damaged at about  $D_0 = 300 \text{ J cm}^{-2}$ , which was lower than  $D_{th}$ , and no perivascular damage occurred at this incident dosage.

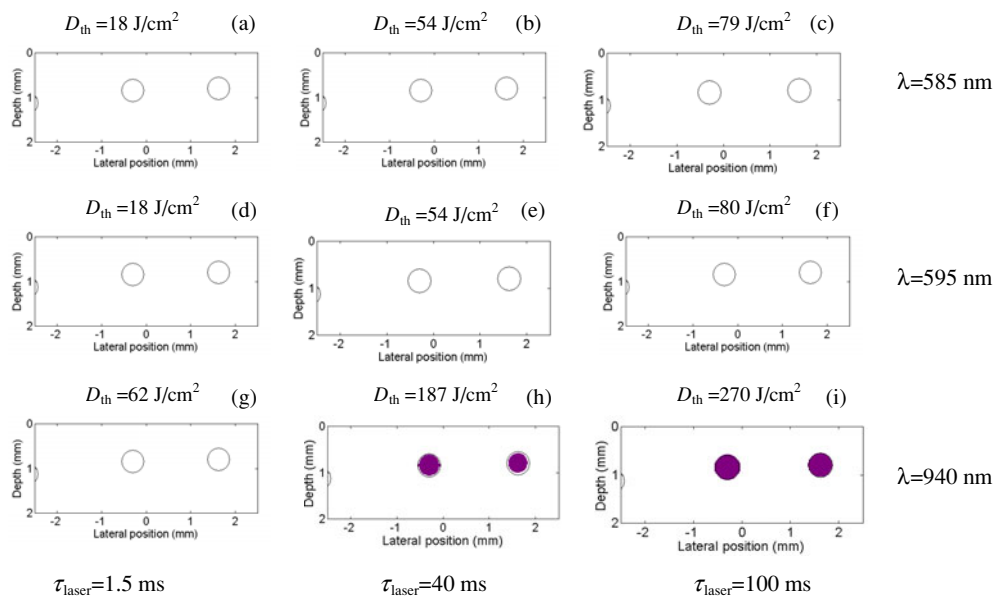


**Figure 3.** Comparison of thermal damage to blood vessel in response to 585 nm ((a), (b) and (c)), 595 nm ((d), (e) and (f)) and 940 nm ((g), (h) and (i)) irradiations in moderately pigmented skin at the threshold incident dosages for epidermal damage  $D_{th}$ . Blood vessel diameter:  $500 \mu\text{m}$ . Cryogen spurt duration: 100 ms. Laser pulse durations: 1.5 ms ((a), (d) and (g)), 40 ms ((b), (e) and (h)) and 100 ms ((c), (f) and (i)). Circled areas: blood vessels; dark areas: damaged regions of blood vessels.

**3.2.2. Moderately pigmented skin.** The corresponding simulation results for moderately pigmented skin are given in figure 3. When irradiated at 585 and 595 nm wavelengths, no blood vessel damage occurred at any of the laser pulse durations from 1.5–100 ms (figures 3(a)–(f)). At 940 nm, almost complete blood vessel damage was predicted when the laser pulse duration reached 100 ms (figure 3(i)).

**3.2.3. Heavily pigmented skin.** In heavily pigmented skin, blood vessel damage did not occur in response to 585 and 595 nm irradiations regardless of the pulse durations from 1.5–100 ms when the corresponding incident dosages for epidermal damage  $D_{th}$  were applied (figures 4(a)–(f)). At 940 nm, only little blood vessel damage was predicted when  $\tau_{laser} = 100$  ms (figure 4(g)). However, when the laser pulse duration was further increased to 200 ms, and the cryogen spurt duration to 200 ms, the blood vessels were almost fully damaged when irradiated at 940 nm (figure 5(c)). In the meantime, still no vascular damage was predicted at 585 and 595 nm under the same conditions (figures 5(a) and (b)).

### 3.3. Blood vessel damage—small-sized blood vessels

**3.3.1. Lightly pigmented skin.** Figure 6 shows the blood vessel damage maps in lightly pigmented skin for  $50 \mu\text{m}$  diameter blood vessels, representing small-sized targets. All simulations were computed at  $D_{th}$  and  $\tau_{CSC} = 100$  ms. With  $\tau_{laser} = 1.5$  ms, 585 nm wavelength induced deeper blood vessel damage depth (figure 6(a), dark areas and arrows indicate damaged regions) than 595 and 940 nm (figures 6(c) and (e)). When  $\tau_{laser}$  was increased to 40 ms, blood vessel damage depth decreased at 585 nm (figure 6(b)), and no vessel damage was found at 595 and 940 nm (figures 6(d) and (f)).

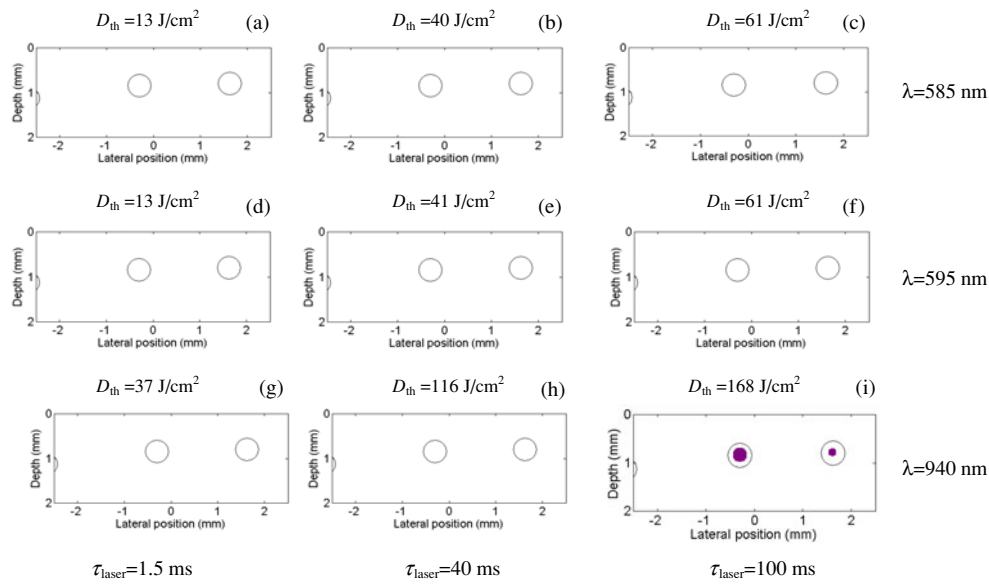


**Figure 4.** Comparison of thermal damage to blood vessel in response to 585 nm ((a), (b) and (c)), 595 nm ((d), (e) and (f)) and 940 nm ((g), (h) and (i)) irradiations in heavily pigmented skin at the threshold incident dosages for epidermal damage  $D_{th}$ . Blood vessel diameter:  $500 \mu\text{m}$ . Cryogen spurt duration: 100 ms. Laser pulse durations: 1.5 ms ((a), (d) and (g)), 40 ms ((b), (e) and (h)) and 100 ms ((c), (f) and (i)). Circled areas: blood vessels; dark areas: damaged regions of blood vessels.

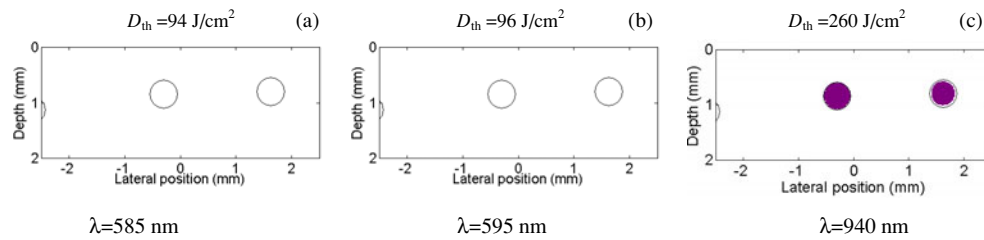


**Figure 5.** Comparison of thermal damage to blood vessel in response to (a) 585 nm, (b) 595 nm and (c) 940 nm irradiations in heavily pigmented skin at the threshold incident dosages for epidermal damage  $D_{th}$ . Blood vessel diameter:  $500 \mu\text{m}$ . Cryogen spurt duration: 200 ms. Laser pulse duration: 200 ms. Circled areas: blood vessels; dark areas: damaged regions of blood vessels.

**3.3.2. Moderately pigmented skin.** For moderately pigmented skin, with  $\tau_{laser} = 1.5$  ms, damage was predicted in the two most superficial blood vessels at 585 nm wavelength (figure 7(a)), while no damage occurred at 595 and 940 nm (figures 7(c) and (e)). When the  $\tau_{laser}$  was increased to 40 ms, no blood vessel damage was found at any of the wavelengths regardless of the pulse durations (figures 7(b), (d) and (f)).

**3.3.3. Heavily pigmented skin.** For heavily pigmented skin, when the incident dosages for epidermal damage  $D_{th}$  (table 5) were applied, blood vessel damage did not occur at any of the wavelengths 585, 595 and 940 nm, and laser pulse durations 1.5 and 40 ms.

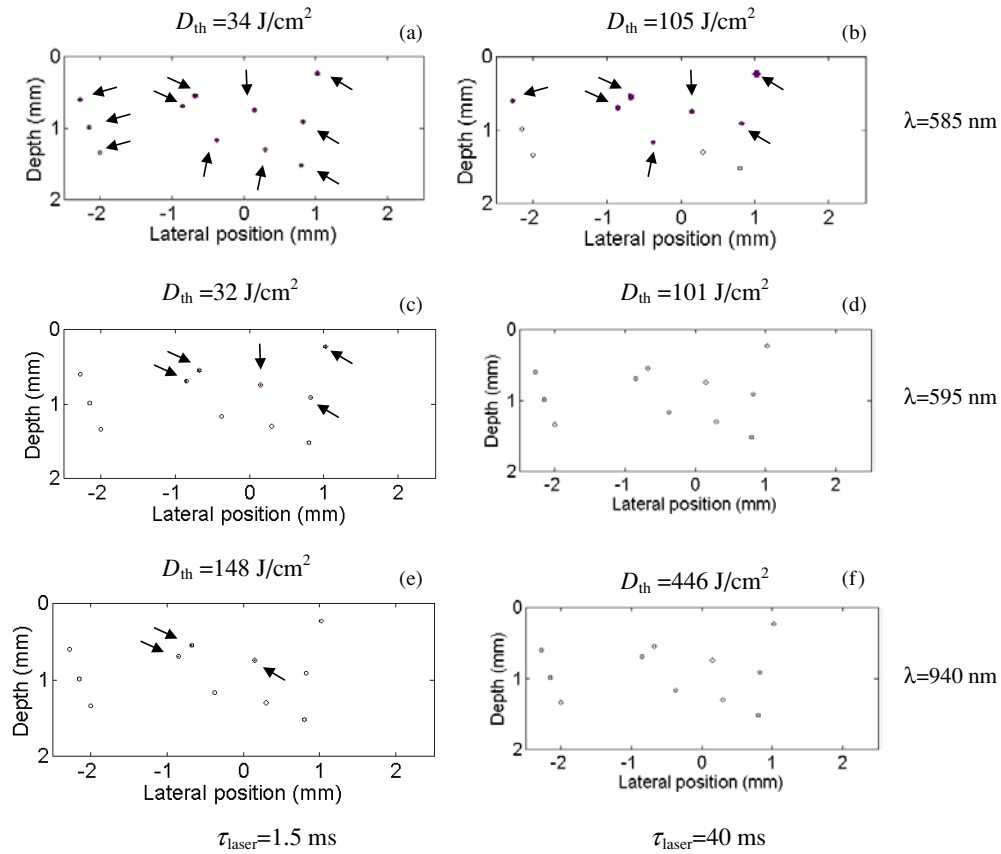


**Figure 6.** Comparison of thermal damage to blood vessel in response to 585 nm ((a) and (b)), 595 nm ((c) and (d)) and 940 nm ((e) and (f)) irradiations in lightly pigmented skin at the threshold incident dosages for epidermal damage  $D_{th}$ . Blood vessel diameter: 50  $\mu\text{m}$ . Cryogen spurt duration: 100 ms. Laser pulse durations: 1.5 ms ((a), (c) and (e)), 40 ms ((b), (d) and (f)). Circled areas: blood vessels; dark areas and arrows: damaged regions of blood vessels.

**Table 5.** Threshold incident dosages for epidermal damage  $D_{th}$  ( $\text{J cm}^{-2}$ ) in heavily pigmented skin.

Wavelength (nm)	Laser pulse duration (ms)	
	1.5	40
585	13 ( $\text{J cm}^{-2}$ )	41 ( $\text{J cm}^{-2}$ )
595	13	40
940	34	108

### 3.4. Effect of dermal blood content

The simulation results for the effect of dermal blood content on the laser-induced peak temperature at the basal layer of epidermis are presented in figure 8(a). The irradiation wavelength was 940 nm, the incident dosage 100  $\text{J cm}^{-2}$ , the cryogen spurt duration 100 ms and the blood vessel size was 500  $\mu\text{m}$  in diameter. Lower dermal blood content led to higher

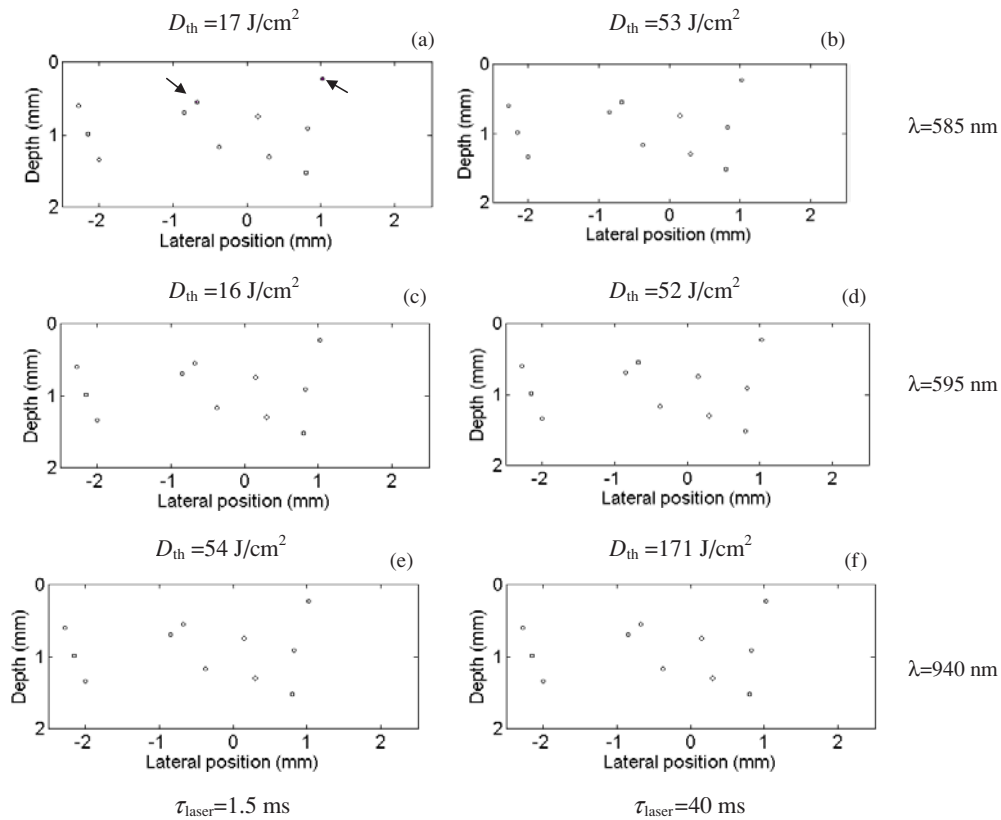


**Figure 7.** Comparison of thermal damage to blood vessel in response to 585 nm ((a) and (b)), 595 nm ((c) and (d)) and 940 nm ((e) and (f)) irradiations in moderately pigmented skin at the threshold incident dosages for epidermal damage  $D_{\text{th}}$ . Blood vessel diameter: 50  $\mu\text{m}$ . Cryogen spurt duration: 100 ms. Laser pulse durations: 1.5 ms ((a), (c) and (e)), 40 ms ((b), (d) and (f)). Circled areas: blood vessels; dark areas and arrows: damaged regions of blood vessels.

laser-induced epidermal peak temperature. At the laser pulse duration of 1.5 ms, the laser-induced epidermal peak temperature increased from 130 to 156  $^{\circ}\text{C}$  when the dermal blood content decreased from 12% to 0.2%. When 100 ms pulse duration was applied, the peak temperatures were 24 and 28.5  $^{\circ}\text{C}$ , respectively.

Accordingly, the threshold incident dosage for epidermal damage  $D_{\text{th}}$  increased with increasing dermal blood content (figure 8(b)). At 1.5 ms pulse duration,  $D_{\text{th}}$  increased from 54 to 65  $\text{J cm}^{-2}$  (20.3% increase) when the dermal blood content increased from 0.2% to 12%. When  $\tau_{\text{laser}} = 100$  ms, the threshold incident dosages were 238 and 280  $\text{J cm}^{-2}$  (17.6% increase) for 0.2% and 12% dermal blood contents, respectively.

### 3.5. Effect of dermal blood vessel size

The simulation results showed that when the dermal blood content is constant, the effect of blood vessel size on the epidermal peak temperature and accordingly the threshold incident dosage for epidermal damage is minimal compared to that of dermal blood content (figure 9). For the example of  $\tau_{\text{laser}} = 1.5$  ms, the threshold incident dosage for epidermal damage

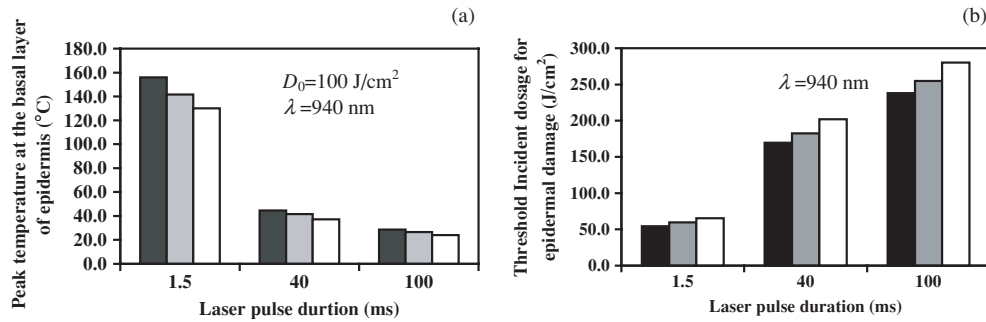


**Figure 8.** Effect of dermal blood content on: (a) the laser-induced temperature at the basal layer of epidermis (incident dosage  $D_0 = 100 \text{ J cm}^{-2}$ ), and (b) the threshold incident dosage for epidermal damage  $D_{th}$ . Dermal blood content: ■ 0.2% ■ 3% □ 12%.

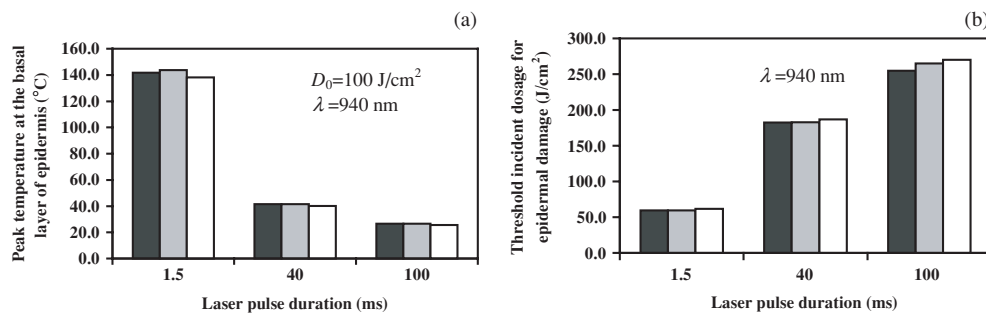


**Figure 9.** Effect of dermal blood vessel size on: (a) the laser-induced temperature at the basal layer of epidermis (incident dosage  $D_0 = 100 \text{ J cm}^{-2}$ ), and (b) the threshold incident dosage for epidermal damage  $D_{th}$ . Blood vessel size ( $\mu\text{m}$ ): ■ 50 ■ 150 □ 500.

increased from  $59.6$  to  $61.5 \text{ J cm}^{-2}$  (3.2% increase only) while the dermal blood size increased from  $50$  to  $500 \mu\text{m}$  (figure 9(b)).

### 3.6. Effects of single continuous laser pulse versus micropulse-composed laser pulse profile

Figure 10 presents the comparison of the thermal effects between single continuous pulse and micropulse-composed pulse profiles. V-beam<sup>TM</sup> laser (Candela Corporation, Wayland, MA) was used as an example of the micropulse-composed profiles for calculation here. The macro pulse delivered by the V-beam<sup>TM</sup> laser is composed of a series of  $100 \mu\text{s}$  duration micro pulses with equal intervals in between. For macro pulses of  $\tau_{\text{laser}} = 1.5\text{--}3 \text{ ms}$ , three micro pulses are present at the intervals of  $\tau_{\text{laser}}/2$ . For  $6\text{--}40 \text{ ms}$  macro pulses, four micro pulses are present at the intervals of  $\tau_{\text{laser}}/3$ . The wavelength used in the calculation was  $595 \text{ nm}$ , macro pulse incident dosage  $20 \text{ J cm}^{-2}$ , cryogen spurt duration  $100 \text{ ms}$  and moderate pigmentation. Figure 10(a) shows the temporal profiles of the temperatures at the basal layer of epidermis in response to the irradiations of the two types of pulse profiles at the same macropulse duration of  $30 \text{ ms}$  preceded by  $100 \text{ ms}$  cryogen spurts. In figure 10(b), the comparison of the peak temperatures at the basal layer of epidermis in response to the irradiations of the two types of pulse profiles at various macropulse durations preceded by  $100 \text{ ms}$  cryogen spurts is presented. For the same macropulse duration and incident dosage, micropulse-composed

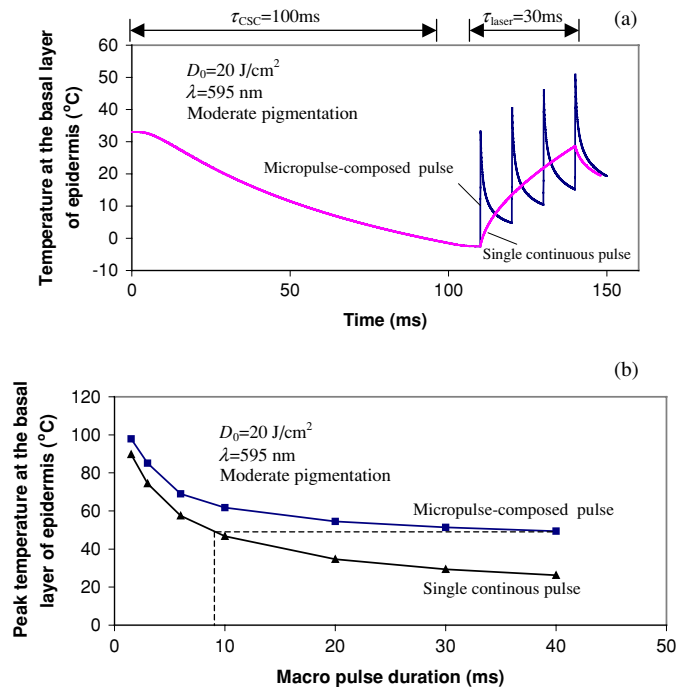


**Figure 10.** Comparison of human skin thermal response to single continuous pulse and micropulse-composed pulse profiles. (a) Temporal profiles of laser-induced temperatures at the basal layer of epidermis in response to the irradiations of the two types of pulse profiles; (b) comparison of the laser-induced peak temperatures at the basal layer of epidermis at various macropulse durations.

profiles result in higher laser-induced peak temperatures in the basal layer of skin epidermis, and the longer the pulse duration, the larger the difference in laser-induced peak temperatures between the two types of laser pulse profiles. With  $\tau_{laser} = 1.5 \text{ ms}$ , the laser-induced peak temperatures at the basal layer of epidermis were 97.9 and 89.7 °C for micropulse-composed pulse and single continuous pulse, respectively. When the pulse duration was increased to 40 ms, the laser-induced peak temperatures were respectively 49.4 and 26.2 °C. In terms of laser-induced peak temperature in skin epidermis, a 40 ms macro pulse delivered by the V-beam™ is approximately equivalent to a 9 ms ideal single continuous pulse (figure 10(b), dashed line).

#### 4. Discussion

The results of this theoretical study demonstrated that the optical selectivity could still be achieved at 940 nm wavelength. The absorption coefficient in blood at 940 nm is about 25 times higher than that in dermis (table 1). Unlike the pronounced gradient of light energy absorption in large-sized blood vessels at 585 and 595 nm wavelengths, the light energy distribution at 940 nm is approximately uniform within the blood vessel (Dai *et al* 2004). This will give rise to more uniform heating of the blood vessel, and subsequently will be beneficial to the photocoagulation of the entire blood vessel. This also explains why pulsed dye lasers are inefficient in treating large-sized ectatic blood vessels. Most of the energy of pulsed dye laser irradiation, especially at 585 nm wavelength, is absorbed by very superficial layer of the

blood vessel. Thus, the light penetration depth in blood is very limited, and subsequently, non-uniform heating of the blood vessel is induced.

The 595 nm wavelength is now widely used in clinical settings with the intention of increasing the light penetration depth in large-sized blood vessels or blood vessels extending deeply into dermis. As the light absorption by blood at 595 nm decreases by a factor of 5 compared with 585 nm (Van Gemert *et al* 1995), higher incident dosages are required to generate sufficient heat within blood vessels for coagulation. However, the light absorption by epidermal melanin at 595 nm is almost identical to that at 585 nm, limiting the usage of high incident dosage and resulting in a poor treatment efficacy in moderately to heavily pigmented skin patients. A comprehensive comparison of the treatment efficacies for large-sized blood vessels among 585, 595 and 940 nm wavelengths was carried out in the present study.

For lightly pigmented skin, in which epidermal melanin plays a less critical role, 940 nm wavelength shows an advantage over 585 and 595 nm in the photocoagulation depth in larger-sized blood vessels (figure 2). For moderately to heavily pigmented skin, 585 and 595 nm wavelengths are constrained by the epidermal light absorption even in conjunction with long cryogen spurt. In contrast, when long laser pulse duration (e.g. 200 ms) and long cryogen spurt duration (e.g. 200 ms) are applied, 940 nm even shows good efficacy in treating large-sized blood vessels in heavily pigmented skin (figure 5).

To achieve selective photothermolysis, laser-induced heat generation should be confined within the targeted blood vessels. To satisfy this, it is suggested that laser pulse duration should be less than the thermal relaxation time of the targeted blood vessel (Anderson and Parrish 1983). However, the original concept of the thermal relaxation time is based on the assumption that the baseline temperature distribution within the target has a Gaussian profile. This is not true especially for large-sized blood vessel irradiated at 585 or 595 nm wavelength. As most of the light energy is only absorbed by the superficial part rather than the whole body of the blood vessel, the 'effective' size of the blood vessel is much smaller than its actual size, and therefore, the 'effective' thermal relaxation time is much shorter than the theoretically calculated one. The simulation results in present study showed that perivascular damage occurred at 585 and 595 nm wavelengths when the pulse durations were between 40 and 100 ms (figures 2(b), (c) and (f)). This indicated that heat was not successfully confined within the targeted blood vessels during the laser irradiation. Using

$$\tau_r = d^2/(16\alpha) \quad (13)$$

where  $\tau_r$  is the theoretical thermal relaxation time (s),  $d$  the blood vessel diameter (m), and  $\alpha$  ( $=1.23 \times 10^{-7} \text{ m}^2 \text{ s}^{-1}$ ) the thermal diffusivity of blood, the theoretical thermal relaxation time is 127 ms for a 500  $\mu\text{m}$  diameter blood vessel. Although the pulse durations used above were shorter than 127 ms, heat was not confined within the targets because of the much shorter 'effective' thermal relaxation time.

In contrast to the results of large-sized blood vessels, 585 nm wavelength shows superior efficacy in treating small-sized blood vessels compared to 940 and 595 nm. In addition, shorter pulse duration (1.5 ms) results in larger blood vessel coagulation depth than longer pulse duration (40 ms). This is consistent with the theory that the pulse duration must match the thermal relaxation time of the targeted blood vessel (Nelson *et al* 1995). For a 50  $\mu\text{m}$  blood vessel,  $\tau_r = 1.27$  ms, which is close to the shorter pulse duration of 1.5 ms. The light penetration depth in blood at 585 nm wavelength is approximately 46  $\mu\text{m}$  ( $1/\mu_a$ ), indicating that almost the whole body of 50  $\mu\text{m}$  blood vessels can be heated. Therefore, the thermal relaxation theory can be applied correctly.

Dermal blood content has a considerable effect on the threshold incident dosage for epidermal damage. Lower dermal blood content leads to less light absorption by dermal blood

and subsequently more back-scattering from the dermis to the epidermis, resulting in higher laser-induced peak temperature in the basal layer, and accordingly, lower threshold incident dosage for epidermal damage. The laser-induced epidermal peak temperature is predicted to be minimally dependent on the size of dermal blood vessels.

The present study was based on the assumption of constant optical properties of human skin during the laser irradiation. Recent studies (Randeberg *et al* 2004, Black and Barton 2004) suggested that changes in optical properties of blood do occur during the laser irradiation due to the thermally induced formation of methaemoglobin from haemoglobin. However, as a first step towards accounting for those changes, a valid functional relationship needs to be determined, and an appropriate mathematical model needs to be adopted for that.

In summary, this theoretical investigation predicted that near-infrared wavelength 940 nm is promising in treating cutaneous hyper-vascular malformation patients with large-sized ectatic blood vessels and moderately to heavily pigmented skin types. On the other hand, 585 nm wavelength results in superior damage of small-sized blood vessels. Future studies are needed to compare present simulations with the large body of experimental results published for laser treatments at all wavelengths considered in this study.

## 5. Conclusions

This theoretical investigation indicated that laser irradiation using 940 nm wavelength is superior to 585 and 595 nm for the treatment of cutaneous hyper-vascular malformation patients with large-sized blood vessels and moderately to heavily pigmented skin types. Using a long laser pulse duration preceded by a long cryogen spurt, 940 nm wavelength is predicted to be effective in treating dark skin patients. On the other hand, 585 nm wavelength shows the best efficacy in treating small-sized blood vessels. Dermal blood content has a considerable effect on the threshold incident dosage for epidermal damage, while the effect of blood vessel size is minimal when the dermal blood content is constant. For the same pulse duration and incident dosage, micropulse-composed pulses result in higher peak temperatures at the basal layer of skin epidermis than ideal single continuous pulses.

## Acknowledgments

This study was supported in part by a grant from the Institute of Arthritis and Musculoskeletal and Skin Disease (IR01-AR47996) at the National Institutes of Health to Dr Bahman Anvari. We thank Dr James W Tunnell from G R Harrison Spectroscopy Laboratory at Massachusetts Institute of Technology for fruitful discussions.

## References

- Agah R, Peach J A, Welch A J and Motamedi M 1994 Rate process model for arterial tissue thermal damage: implications on vessel photocoagulation *Lasers Surg. Med.* **15** 176–84
- Aguilar G, Majaron B, Pope K, Svaasand L O, Lavernia E J and Nelson J S 2001 Influence of nozzle-to-skin distance in cryogen spray cooling for dermatologic laser surgery *Lasers Surg. Med.* **28** 113–20
- Anderson R R and Parrish J A 1983 Selective photothermolysis: precise microsurgery by selective absorption of pulsed radiation *Science* **220** 524–7
- Ashinoff R and Geronemus R G 1992 Treatment of a port wine stain in a black patient with pulsed dye laser *J. Dermatol. Surg. Oncol.* **18** 147–8
- Anvari B, Milner T E, Tanenbaum B S, Kimel S, Svaasand L O and Nelson J S 1995 Selective cooling of biological tissues: application for thermally mediated therapeutic procedures *Phys. Med. Biol.* **40** 241–52

- Black J F and Barton J K 2004 Chemical and structure changes in blood undergoing laser photocoagulation *Photochem. Photobiol.* **80** 89–97
- Buscher B A, Mcmeekin T O and Goodwin D 2000 Treatment of telangiectasia by using a long-pulse dye laser at 595 nm with and without dynamic cooling device *Lasers Surg. Med.* **27** 171–5
- Dai T, Pikkula B M, Wang L V and Anvari B 2004 A theoretical investigation of human skin thermal response to near-infrared laser irradiation *Proc. SPIE* **5312** 7–17
- Duck F A 1990 *Physical Properties of Tissue* (London: Academic)
- Fitzpatrick T B 1988 The validity and practicality of sun-reactive skin types I through VI *Arch. Dermatol.* **124** 869–71
- Graaff R, Dassel A C M, Koelink M H, de Mul F F M, Aarnoudse J G and Zijlstra W G 1993 Optical properties of human dermis *in vitro* and *in vivo* *Appl. Opt.* **32** 435–47
- Ho W S, Chan H H, Ying S Y and Chan P C 2002 Laser treatment of congenital facial port-wine stains: long-term efficacy and complication in Chinese patients *Lasers Surg. Med.* **30** 44–7
- Hohenleutner S, Badur-Ganter E, Landthaler M and Hohenleutner U 2001 Long-term results in the treatment of childhood hemangioma with the flashlamp-pumped pulsed dye laser: an evaluation of 617 cases *Lasers Surg. Med.* **28** 273–7
- Incropera F P and Dewitt D P 2001 *Fundamentals of Heat and Mass Transfer* (New York: Wiley)
- Jacques S L 1998 *Skin Optics* <http://omlc.ogi.edu/news/jan98/skinoptics.html>
- Kaudewitz P, Klövekorn W and Rother W 2001 Effective treatment of leg vein telangiectasia with a new 940 nm diode laser *Dermatol. Surg.* **27** 101–6
- Kienle A and Hibst R 1995 A new optimal wavelength for port wine stain? *Phys. Med. Biol.* **40** 1559–76
- Lanigan S W 1998 Port-wine stains unresponsive to pulsed dye laser: explanations and solutions *Br. J. Dermatol.* **139** 173–7
- Nelson J S, Minler T E, Svaasand L O and Kimel S 1995 Laser pulse duration must match the estimated thermal relaxation time for successful photothermolysis of blood vessels *Lasers Med. Sci.* **10** 9–12
- Nguyen C M, Yohn J J, Huff C, Weston W L and Morelli J G 1998 Facial port wine stains in childhood: prediction of the rate of improvement as a function of the age of the patient, size and location of the port wine stain and the number of treatments with the pulsed dye (585 nm) laser *Br. J. Dermatol.* **138** 821–5
- Randeborg L L, Bonesronning J H, Dalaker M, Nelson J S and Svaasand L O 2004 Methemoglobin formation during laser induced photothermolysis of vascular skin lesion *Lasers Surg. Med.* **34** 414–9
- Roggan A, Dorschel K, Minet O, Wolff D and Muller G 1995 The optical properties of biological properties in the near infrared wavelength range—review and measurements *Laser-Induced Interstitial Thermotherapy* ed G Muller and A Roggan (Bellingham: SPIE Press) pp 10–44
- Roggan A, Friebel M, Dorschel K, Hahn A and Muller G 1999 Optical properties of circulating human blood in the wavelength range 400–2500 nm *J. Biomed. Opt.* **4** 36–46
- Torres J H, Nelson J S, Tanenbaum B S, Milner T, Goodman D M and Anvari B 1999 Estimation of internal skin temperatures in response to cryogen spray cooling: implications for laser therapy of port wine stains *IEEE J. Sel. Top. Quantum Electron* **5** 1058–66
- Torres J H, Tunnell J W, Pikkula B M and Anvari B 2001 An analysis of heat removal during cryogen spray cooling and effects of simultaneous airflow application *Lasers Surg. Med.* **28** 477–86
- Tunnell J W, Torres J H and Anvari B 2002 Methodology for estimation of time-dependent surface heat flux due to cryogen spray cooling *Ann. Biomed. Eng.* **30** 19–33
- Tunnell J W, Wang L V and Anvari B 2003a Optimum pulse duration and radiant exposure for vascular laser therapy of dark port-wine skin: a theoretical study *Appl. Opt.* **42** 1367–78
- Tunnell J W, Chang D W, Johnston C, Torres J H, Jr Patrick C W, Miller M J, Thomsen S L and Anvari B 2003b Effects of cryogen spray cooling and high radiant exposures on selective vascular injury during laser irradiation of human skin *Arch. Dermatol.* **139** 743–50
- Van Gemert M J C, Welch A J, Pickering J W and Tan O T 1995 Laser treatment of port wine stains *Optical-Thermal Response of Laser-Irradiated Tissue* ed A J Welch and M J C van Gemert (New York: Plenum) pp 789–830
- Wang L, Jacques S L and Zheng L 1995 MCML-Monte Carlo modeling of light transport in multi-layered tissues *Comput. Methods Programs Biomed.* **47** 131–46
- Weaver J A and Stoll A M 1969 Mathematical model of skin exposed to thermal radiation *Aerosp. Med.* **40** 24–30